X-ray-diffraction study of size-dependent strain in quantum-wire structures

Qun Shen and Stefan W. Kycia
Cornell High Energy Synchrotron Source (CHESS), Cornell University, Ithaca, New York 14853

E. S. Tentarelli, W. J. Schaff, and L. F. Eastman
School of Electrical Engineering, Cornell University, Ithaca, New York 14853

(Received 11 September 1996)

We report a synchrotron x-ray-diffraction study of the strain field in embedded $In_{0.2}Ga_{0.8}As/GaAs$ (001) quantum wires of widths 50–250 nm. Our results show a size-dependent orthorhombic lattice deformation in the wires and a linearly strained interfacial region near the wire sidewalls. The measured strain is responsible for an unusual band-gap energy increase that is several times larger than the quantum confinement effect, indicating that strain effects contribute significantly to band-edge energies in this and other quantum structures. [S0163-1829(96)00948-4]

Quantum confinement in low-dimensional semiconductor materials has attracted much interest in recent years because of its fundamental connection to quantum and solid-state physics and its potential impact on semiconductor electronic and optoelectronic devices.[1] These materials are categorized into three types: quantum wells, quantum wires (QWR's), and quantum dots (QD's), in which the electron motions are restricted to two, one, and zero dimensions, respectively. For a strong confinement effect to occur, the dimension of the crystal needs to approach its exciton radius which is on the order of 10 nm. This typical dimension of the quantum confinement materials, which may contain only a few dozens atoms in each direction, represents an intermediate (mesoscopic) length scale that is different from dimensions studied in conventional macroscopic and microscopic physics. Some physical properties, such as electron transport and electronic band structures, may be significantly modified compared to the corresponding bulk materials, leading to different mesoscopic effects.

One of the main effects of quantum confinement is the widening of the forbidden band gap in direct-gap semiconductors such as III-V compounds. Optical spectroscopic techniques such as photoluminescence (PL) are often used to measure the increase in the band gap as a function of decreasing crystal sizes. For lateral QWR and QD structures, quantitative observations of the band-gap change versus confinement size have become available recently, owing to the improvement in the control of small lateral dimensions in lithographic processes.[2,3] These quantitative analyses, however, often exhibit significant discrepancies between the theory and the experiment. For example, blueshifts in PL peak energy several times greater than the quantum confinement predictions have been observed in embedded QWR's of $In_xGa_{1-x}As/GaAs$ (Refs. 3, 4) and of $In_xAs_{-x}P/InP$.[5] The discrepancies remain unresolved even if improved lateral confinement theories are used in which such effects as the band anisotropy, nonparabolicity, and subband mixing are included.[2,5,6]

It has become clear that one important factor that can affect the laterally confined electronic properties is the state of crystalline strain in the QWR and QD structures, as suggested by the observations that the large blueshift discrepancies seem to exist only for QWR's and QD's with a lattice-mismatched cap layer.[4,5] Several studies based on the continuum elasticity theory have also suggested the importance of strain in QWR's and QD's and their influence on the band-gap energy.[5,7,8] Experimentally, however, there have been very few studies that provide direct measurements of strain-tensor components in lateral quantum structures as a function of quantum-wire width, w, primarily because of the difficulties in measuring the small amount of strain in small crystals with sufficient accuracy.[4,9]

In this paper, we report a direct measurement by synchrotron x-ray diffraction of the elastic strain tensor and strain gradient in embedded periodic $In_{0.2}Ga_{0.8}As/GaAs$ QWR structures of several lateral sizes. In our experiment, we make use of the constructive interference among the QWR's within the coherence width of the synchrotron x-ray beam. This phenomenon of *coherent grating x-ray diffraction* enhances the scattering signal from individual wires, and thus significantly improves the strain detectibility by x-ray diffraction.[10–12] Our measured strain components in the QWR's show a size-dependent orthorhombic deviation from the tetragonal pseudomorphic deformation usually associated with quantum wells. The orthorhombic lattice strain does not seem to be a simple result of the elastic Poisson effect previously discussed for uncapped and much thicker QWR's.[7] Finally, we use the standard deformation-potential theory[13] to show that the confinement potential in the QWR's are modified substantially by the measured strain field, causing the extra blueshifts observed in the PL measurement.

X-ray diffraction from a periodic QWR array, which acts like a grating with a submicrometer period, L, consists of superlattice peaks around each Bragg reflection, **G**, of the internal QWR crystal lattice. The diffracted x-ray intensities of the superlattice peaks are given by[14]

$$I(\mathbf{q}) = |f_p(\mathbf{q})|^2 \left[\frac{\sin(Nq_xL/2)}{\sin(q_xL/2)}\right]^2, \tag{1}$$

where $f_p(\mathbf{q})$ is the scattering amplitude from a single period, NL the coherence length of the x-ray beam, and **q** is the

momentum transfer measured from **G**. The grating superlattice diffraction peaks occur at intervals $\Delta q_x = 2\pi/L$ and their intensities are determined by the geometric profile and the internal crystalline strain within a single period.

The QWR samples of 10-nm-thick $In_{0.2}Ga_{0.8}As$, embedded in a GaAs (001) substrate, were fabricated on a single GaAs wafer by a combination of molecular-beam epitaxy, electron-beam lithography, and epitaxial regrowth techniques.[3] The QWR's are along the [110] direction (inset in Fig. 1) with wire widths ranging from $w = 50$ to 900 nm, as measured by scanning electron microscopy. Each patterned QWR area was 0.7×0.7 mm^2. The PL measurements were carried out at room temperature using an Ar^+ laser of a 514.5-nm wavelength. Blueshifts in the PL peak energy versus QWR widths were observed on this and other similarly made samples. It was found consistently that the energy shifts were several times greater than the expected values due solely to the quantum confinement effect.[3,4]

The x-ray-diffraction experiment was performed at the A2 station of CHESS, using 8.33-keV x rays provided by horizontally focused Si (111) monochromators. The QWR sample was mounted at the center of a standard four-circle diffractometer equipped with a post-sample Si (111) analyzer. The incident beam, about 1 by 0.5 mm in size, covers a sample surface area about twice as large as each patterned QWR region at typical diffraction geometries. Bragg-reflection topographs were taken to ensure that only one patterned area with a given QWR width was illuminated by the x-ray beam for each measurement.

The strain measurements on five QWR regions of wire widths 50, 70, 90, 130, and 250 nm were performed by mesh scans around the symmetric (004) and the asymmetric (115) Bragg reflections of $In_{0.2}Ga_{0.8}As$. An example of the diffraction patterns is shown in Fig. 1, where sharp superlattice peaks and clear extinctions of certain orders indicate an almost perfect QWR array with very little size variation. The (115) reflection was useful for measuring the *average* strain tensor in a QWR, while the diffraction pattern around the (004) proved to be extremely sensitive to the *spatial distribution* of the strain field near the QWR sidewalls.

Two groups of QWR superlattice peaks are visible in the (115) diffraction pattern in Fig. 1, one around the (115) reflection of GaAs and the other around the (115) of $In_{0.2}Ga_{0.8}As$. The strong (115) peak of the $In_{0.2}Ga_{0.8}As$, positioned directly below the GaAs (115), comes mainly from the unpatterned region of the sample. It indicates a pseudomorphically strained thin layer of $In_{0.2}Ga_{0.8}As$, with a thickness of 100 Å, whose lateral lattice is conformed to the substrate. The separation in q_z between the two (115) reflections corresponds to a lattice difference of 2.74% ($a^{GaAs} = 5.653$ Å, $a_z^{In_xGa_{1-x}As} = 5.808$ Å), which is consistent with a lattice mismatch of 1.4% between the two bulk materials and an elastic Poisson's factor of $\sigma = -2C_{12}/C_{11} = -0.933$, where C_{11} and C_{12} are the elastic constants.

The lateral positions of the $In_{0.2}Ga_{0.8}As$ grating superlattice peaks are perfectly lined up with the unpatterned $In_{0.2}Ga_{0.8}As$ and the GaAs (115) peaks, indicating a commensurate charge-density modulation with respect to the substrate. The QWR's themselves, however, are strained, as indicated by the offset of the grating-peak envelope profile in Fig. 1 with respect to the unpatterned $In_{0.2}Ga_{0.8}As$ (115)

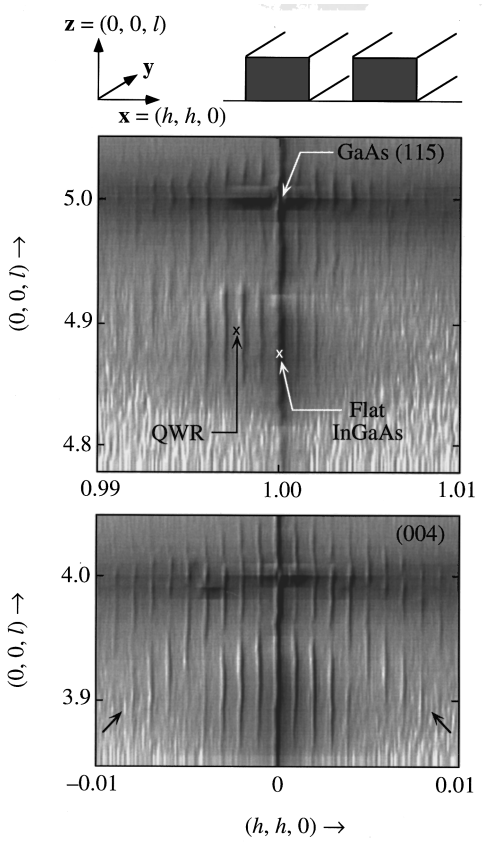

FIG. 1. Intensity surface plots, in logarithmic scale, of the x-ray-diffraction patterns around the (115) and the (004) reflections of the 50-nm-wide QWR sample of $In_{0.2}Ga_{0.8}As/GaAs$. The ''×'' marks in the (115) plot indicate the centers of the diffraction patterns from the QWR and from the unpatterned flat region on the sample, respectively. The tilted arrows in the (004) plot indicate the directions of the strain-gradient-induced diffraction streaks, as explained in the text.

peak. To quantify this additional strain, we fit the measured intensities with the envelope function $|f_p(q_x, q_z)|^2$ being $[\sin(q_x w/2)/(q_x w)]^2$ in q_x and a Gaussian in q_z, respectively. The deviations of the center of the envelope function from the unpatterned (115) peak position are then converted to real-space strain components, ϵ_{xx} and ϵ_{zz}, which are plotted in Figs. 2(a), 2(b). The strain ϵ_{yy} along the QWR direction (**y**) was measured at (115) and was found to be pseudomorphic, $\epsilon_{yy} = 0$, as one may expect.

Several observations can be made on the results shown in Figs. 2(a), 2(b). First, the crystal lattice in the QWR's becomes *orthorhombic* rather than *tetragonal*, since $\epsilon_{xx} \neq \epsilon_{yy}$. This result is consistent with the overall symmetry of the QWR crystals if their boundaries are taken into account. Second, the orthorhombic strain increases significantly with decreasing QWR widths. This dependence, especially that of ϵ_{xx}, is somewhat surprising. Since the total strain energy per unit length of QWR decreases with width, we may expect that a wire with a smaller cross-section area would be easier to conform to the surrounding substrate lattice, and thus only ϵ_{zz} would decrease with width while ϵ_{xx} would remain locked to the substrate. Our measurements clearly show that it is not the case. Third, the relationship between ϵ_{xx} and ϵ_{zz} does not seem to follow the usual elastic Poisson's behavior,

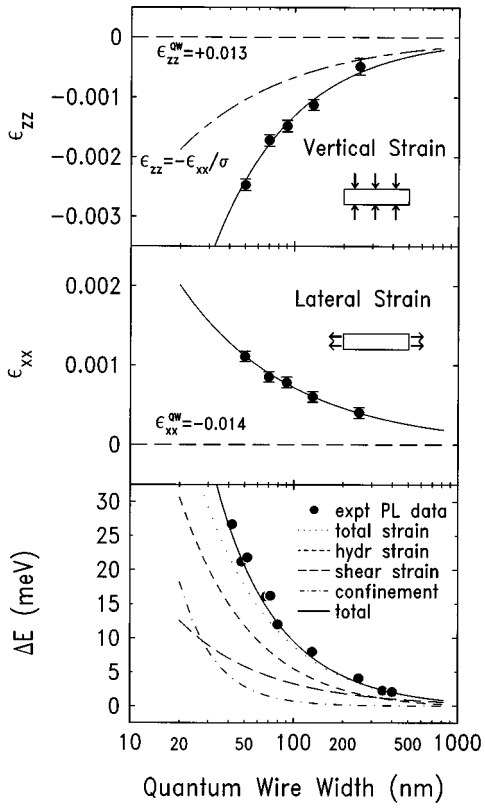

FIG. 2. Measured strain components ϵ_{zz} in (a) and ϵ_{xx} in (b), as a function of QWR width, plotted as the deviations from the pseudomorphic strain (dashed lines) in a quantum film. The solid curves are the power-law fits to the data. The strain-induced band-gap energy change is shown in (c) as the dotted curve. The full circles are the experimental PL data. The dash-dotted curve represents the quantum confinement theory. The sum of the strain and the confinement effects is shown as the solid curve.

as shown by the long-short-dashed curve in Fig. 2(a). This last point demonstrates the complexity of the elasticity behavior of lattice-mismatched QWR systems, and the necessity of the direct experimental strain measurements.

In addition to the *average* strain tensors in the QWR's, we can also obtain from x-ray diffraction the *spatial distribution* of the strain field near the sidewalls. Because of the lattice mismatch in the vertical direction, a transitional region may exist near the sidewalls in which the lattice constant a_z varies with lateral position, x. The specific spatial locations of these transitional regions can produce a unique x-ray interference pattern (envelope function of the grating peaks) that is distinctly different from the ordinary single-wire Fraunhofer diffraction profile.

There are two pronounced features directly related to the strain gradient near the sidewalls. First, there exist broad intensity streaks from the GaAs peak downward but inclined with respect to the q_x and q_z axes. These streaks, indicated by tilted arrows in Fig. 1, are the interference fringes from the two strained sidewall regions located symmetrically at either side of the QWR. The slopes of these streaks are determined by the lateral gradient of the vertical lattice constant, $\partial a_z/\partial x$, and the wire width, w. Second, the single-wire Fraunhofer diffraction profile at the q_z position of $In_{0.2}Ga_{0.8}As$ is significantly modified by the strained sidewall regions. The wire width appears to be larger with the strained region than without. With the help of a computer simulation of the whole diffraction pattern in Fig. 1, we come to the conclusion that at each sidewall there exists a region of $\sim$240 Å in lateral width where the vertical lattice parameter varies linearly with a gradient of $\partial a_z/\partial x=(6.3\pm1.5)\times10^{-4}$. The width of this interfacial region does not change significantly with the QWR's lateral dimensions.

In order to see whether our measured average strain components are consistent with the observed PL blueshift, we use the deformation-potential theory developed by Pikus and Bir[13] to calculate the band-gap change due to the strain: $\Delta E_g=a(\epsilon_{11}+\epsilon_{22}+\epsilon_{33})-\sqrt{\mathcal{E}_\epsilon}$, with $\mathcal{E}_\epsilon=b^2[(\epsilon_{11}-\epsilon_{22})^2+(\epsilon_{22}-\epsilon_{33})^2+(\epsilon_{33}-\epsilon_{11})^2]/2+d^2(\epsilon_{12}^2+\epsilon_{23}^2+\epsilon_{31}^2)$, where a is the hydrostatic and b and d are the shear interband deformation potentials, based on crystallographic axes $\hat{\mathbf{1}}$=[100], $\hat{\mathbf{2}}$=[010], and $\hat{\mathbf{3}}$=[001]. The measured strain components, (ϵ_{xx}, ϵ_{yy}, ϵ_{zz}), based on $\hat{\mathbf{x}}$ along [110], $\hat{\mathbf{y}}$ along [110], and $\hat{\mathbf{z}}$ along [001], are transformed by a 45° rotation around $\hat{\mathbf{z}}$ to yield that $\epsilon_{11}=\epsilon_{22}=\epsilon_{xx}/2$, $\epsilon_{12}=\epsilon_{21}=\epsilon_{xx}/2$, and $\epsilon_{33}=\epsilon_{zz}$. The total strain components with respect to unstrained bulk crystals are therefore $\epsilon_{11}=\epsilon_{22}=-\epsilon_0+\epsilon_{xx}/2$, $\epsilon_{12}=\epsilon_{21}=\epsilon_{xx}/2$, and $\epsilon_{33}=(2C_{12}/C_{11})\epsilon_0+\epsilon_{zz}$, where ϵ_0=0.014 is the lattice mismatch between $In_{0.2}Ga_{0.8}As$ and GaAs. Substituting these strain components into the equation for ΔE_g, we obtain the band-gap change *in addition* to that of the tetragonally strained quantum film (QWR with $w=\infty$):

$$\Delta E=a(\epsilon_{xx}+\epsilon_{zz})+b(\epsilon_{zz}-\epsilon_{xx}/2), \tag{2}$$

where the terms containing second orders of ϵ_{xx} and ϵ_{zz} have been omitted since ϵ_{xx} and ϵ_{zz} are much smaller than ϵ_0.

We use the values $a=-9.016$ eV and $b=-1.96$ eV for the $In_{0.2}Ga_{0.8}As$, which are interpolated between the values for GaAs and InAs.[15] For ϵ_{xx} and ϵ_{zz}, we first fit the measured values with two smooth curves: $\epsilon_{xx}=0.0138w^{-0.64}$ and $\epsilon_{zz}=-0.0738w^{-0.87}$. Then we use these smoothed curves for computation of ΔE using Eq. (2). The total band-gap change is the sum of the strain-induced effect, Eq. (2), and the quantum confinement effect, which can be estimated by using the effective-mass approximation.[15] The result is shown in Fig. 2(c) as a solid curve, along with the measured PL data (full circles) and the pure confinement effect (dash-dotted curve). The calculated ΔE is in excellent agreement with the measured blueshifts, indicating that the strain is the predominant cause of the band-structure changes in these embedded QWR materials.

Also shown in Fig. 2(c) are the separate contributions to ΔE from the hydrostatic strain, $a(\epsilon_{xx}+\epsilon_{zz})$, and from the shear strain, $b(\epsilon_{zz}-\epsilon_{xx}/2)$. It shows that the isotropic hydrostatic compression of the embedded QWR's by the surrounding substrate crystal contributes most to the band gap increase in small-width QWR's. Although the pressure dependence of electronic band structures has been known for bulk semiconductors, our result indicates that the hydrostatic and shear stress from the lattice mismatch in nanocrystallite materials is extremely important in determining their quantum confinement potentials and their optoelectronic properties. This effect may become even more essential for smaller quantum structures, and may be useful for strain engineering of new electronic nanostructures. We should note that for free-standing quantum structures, the natural surface relax-

ation may also be important in determining the electronic properties, especially for small scale structures.

In summary, we have used the coherent grating-enhanced x-ray diffraction to study the strain field in embedded QWR structures of $In_{0.2}Ga_{0.8}As/GaAs$. We have observed an orthorhombic distortion in the QWR's that is lateral-size dependent. This size-dependent strain is the predominant cause for the unusually large blueshift observed in the PL measurement. Our result demonstrates that the elastic strains in lattice-mismatched QWR structures not only affect the materials growth and fabrication but also strongly influence the electronic band edges, confinement potentials, and thus optical properties of the low-dimensional quantum structures. An accurate determination of the strain fields in these ultrasmall structures can provide the crucial information needed for better understanding of their unusual physical properties and better engineering of new mesoscopic materials. Furthermore, in conjunction with other experimental techniques, results from coherent grating x-ray diffraction can be used to assess the applicability of many existing solid-state theories, such as that of elastic deformation potentials, to the regime of mesoscopic low-dimensional structures. These studies in turn may stimulate further theoretical and experimental research in the area of mesoscopic physics.

This work was supported by the National Science Foundation through CHESS under Grant No. DMR-9311772. Work performed at the School of Electrical Engineering was supported by the Office of Naval Research under Contract No. N00014-1-0464.

[1] W. P. Kirk and M. A. Reed, *Nanostructures and Mesoscopic Systems* (Academic, New York, 1992).

[2] M. Notomi, S. Nojima, M. Okamoto, H. Iwamura, and T. Tamanura, Phys. Rev. B **52**, 11 073 (1995).

[3] J. D. Reed, Y.-P. Chen, E. S. Tentarelli, W. J. Schaff, and L. F. Eastman, J. Vac. Sci. Technol. B **13**, 995 (1995).

[4] E. S. Tentarelli, J. D. Reed, Y.-P. Chen, W. J. Schaff, and L. F. Eastman, J. Appl. Phys. **78**, 4031 (1995).

[5] M. Notomi, J. Hammersberg, H. Weman, S. Nojima, H. Sugiura, M. Okamoto, T. Tamamura, and M. Potemski, Phys. Rev. B **52**, 11 147 (1995).

[6] R. Chen and K. K. Bajaj, Phys. Rev. B **50**, 1949 (1994).

[7] L. De Caro and L. Tapfer, Phys. Rev. B **51**, 4381 (1995).

[8] N. A. Gippius, S. G. Tikhodeev, R. Steffen, T. Koch, and A. Forchel, in *Surface/Interface and Stress Effects in Electronic Material Nanostructures*, edited by S. M. Prokes, K. L. Wang, R. C. Cammarata, and A. Christou, MRS Symposium Proceedings No 405 (Materials Research Society, Pittsburgh, 1996), p. 121.

[9] Y.-P. Chen, J. D. Reed, W. J. Schaff, and L. F. Eastman, Appl. Phys. Lett. **65**, 2202 (1994).

[10] Qun Shen, in *Surface/Interface and Stress Effects in Electronic Material Nanostructures* (Ref. 8), p. 371.

[11] L. Tapfer, G. C. Larocca, H. Lage, O. Brandt, D. Heitmann, and K. Ploog, Appl. Surf. Sci. **60**, 517 (1992).

[12] V. Holy, A. A. Darhuber, G. Bauer, P. D. Wang, Y. P. Song, C. M. Sotomayor-Torres, and M. C. Holland, Phys. Rev. B **52**, 8348 (1995).

[13] G. E. Pikus and G. L. Bir, Fiz. Tverd. Tela (Leningrad) **1**, 1642 (1959) [Sov. Phys. Solid State **1**, 1502 (1959)].

[14] Qun Shen, C. C. Umbach, B. Weselak, and J. M. Blakely, Phys. Rev. B **48**, 17 967 (1993).

[15] *Physics of Group IV Elements and III–V Compounds*, edited by K.-H. Hellwege and O. Madelung, Landolt-Börnstein, New Series, Group III, Vol. 17, pt. a (Springer, Berlin, 1982).